Proceedings of 2010 IEEE International Conference on Ultra-Wideband (ICUWB2010)

An Ultra-Wideband Vertical Transition from Microstrip to Stripline in PCB Technology

Mario Leib, Michael Mirbach, and Wolfgang Menzel

University of Ulm, Microwave Techniques, Albert-Einstein-Allee 41, 89081 Ulm, Germany
Email: mario.leib@uni-ulm.de

***Abstract*—An ultra-wideband transition from microstrip to stripline in PCB technology is presented applying only through via holes for simple fabrication. The design is optimized using full-wave EM simulations. A prototype is manufactured and measured achieving a return loss better than 8.7 dB and an insertion loss better than 1.2 dB in the FCC frequency range. A meander-shaped delay line in stripline technique is presented as an example of application.**

***Index Terms*—planar transmission lines, microstrip, stripline, stripline transitions, ultra-wideband (UWB),**

I. Introduction

The transmission of ultra-wideband (UWB) impulses in planar circuits demands for transmission lines with low dispersion and low parasitic radiation. As a real TEM transmission line, the stripline perfectly satisfies these two demands. Especially the frequency independence of its transmission properties makes this type of transmission line very interesting for broadband impulse-based applications such as UWB radar systems. A main application of striplines is found in feeding networks of antennas and in low dispersive delay lines for phased array and radar systems, as for instance the comb filter approach for impulse-radio UWB systems described in [1]. They also appear increasingly in multilayer circuits, in particular in low-temperature cofired ceramic (LTCC) technology. Furthermore, striplines are predestined to be used as feeding transmission lines for antenna structures that already possess a stripline topology such as stripline slot antennas [2], [3].

The usage of striplines usually requires transitions from other types of transmission lines. In order to connect stripline structures to the output of monolithic integrated circuits or to a coaxial connector for characterization purposes, a transition from microstrip line to stripline is needed. Different broadband transitions have been examined in LTCC technology [4]–[6] or on multilayer printed circuit boards (PCB) [7]. However, these concepts require blind vias complicating the fabrication process.

The microstrip-to-stripline transition presented here is designed in PCB technology on two substrate layers applying through via holes instead of blind vias, and therefore allowing an easy fabrication. Similar vertical transitions using via holes have been examined in [8] for PCB multilayer structures. There, however, a via-to-stripline transition applicable for packages and SMA connectors and not a microstrip-to-stripline transition is considered.

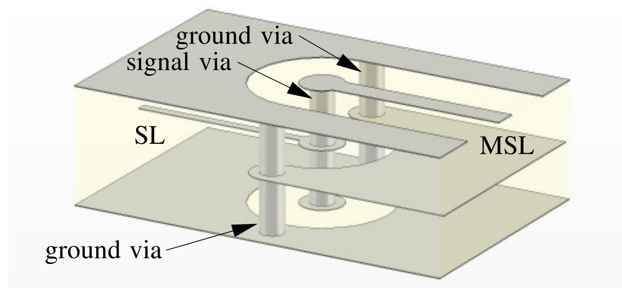

Fig. 1. Sketch of the proposed vertical transition from microstrip line (MSL) to stripline (SL).

II. Design of the Microstrip-to-Stripline Transition

The final design of the vertical microstrip-to-stripline transition (MSL–SL) is shown in Fig. 1. It consists of three metallization layers printed on two layers of dielectric substrate. The $50\,\Omega$ microstrip line is connected to the signal via with a $50\,\Omega$ stripline placed between two ground metallization layers. Two via holes beside the signal via connect the stripline ground metallization layers to the ground plane of the microstrip line. In order to permit a simple fabrication process, via holes penetrating all substrate layers are used. This results in an open-ended stub of the signal via.

First investigations are performed to determine the optimum distance between the three via holes. For this purpose, the characteristic impedance of an ideal three-wire line, surrounded by a material with the permittivity of the substrate, is simulated as a function of the via distance d [9]. The results of these simulations are plotted in Fig. 2, showing that matching to the given $50\,\Omega$ transmission lines is achieved for a via distance of 1.9 mm. This value is used as a starting point for the design of the transition. All simulations in this work are performed with a commercial full-wave field solver [10].

Pads around the vias (see Fig. 1) are mandatory to ensure a proper fabrication of the vias and, hence, guarantee a connection between a printed line and a via hole. However, the size of these annular rings has an effect on the overall behavior of the structure, as it leads to an additional capacitive loading. This effect is examined by simulating the whole transition structure for different pad diameters d_{pad} (cf. Fig. 4).

Fig. 3 shows the simulated return loss of the transition

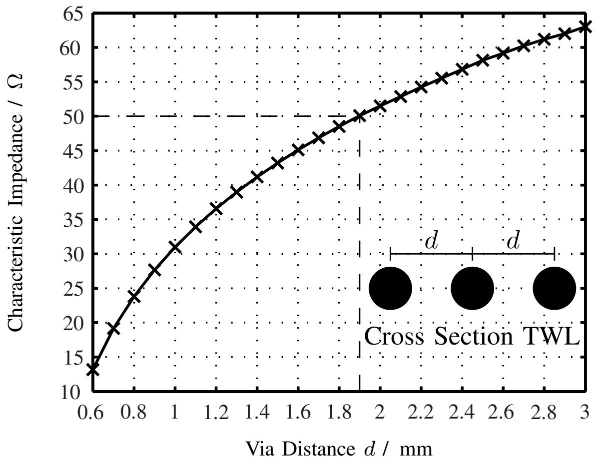

Fig. 2. Characteristic impedance of a simple three-wire line (TWL) as a function of the via distance d. The via diameter is $d_{\mathrm{via}} = 0.5\,\mathrm{mm}$ and the permittivity of the surrounding medium is $\varepsilon_{\mathrm{r}} = 10.2$.

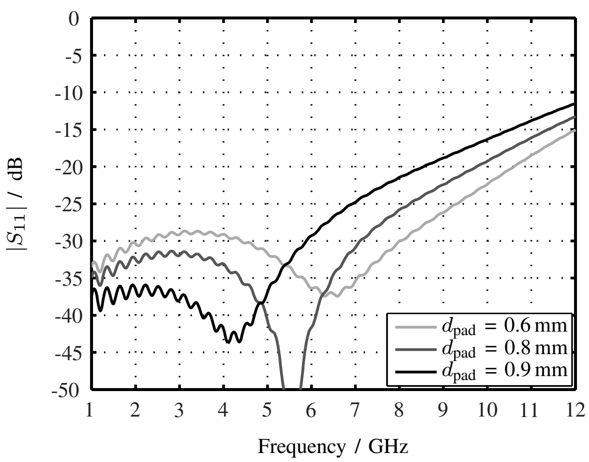

Fig. 3. Simulated return loss of the microstrip-to-stripline transition for different pad diameters d_{pad}.

for three different pad diameters. The resonances at 4.1 GHz, 5.7 GHz and 6.6 GHz are caused by the open-ended stub of the signal via and lead to an improvement of the return loss performance in contrast to a transition applying a blind via [8]. It can also be seen that the capacitive loading of bigger annular rings leads to an increased return loss for higher frequencies. Nevertheless, to ensure proper fabrication a pad diameter of $d_{\mathrm{pad}} = 0.9\,\mathrm{mm}$ was chosen.

In the final realization of the transition laterally placed ground vias every 2 mm ($=\frac{\lambda_{12\,\mathrm{GHz}}}{4}$) are used to suppress parasitic parallel plate modes. Hence, a dielectric-filled waveguide is formed, which could allow the propagation of undesired TE modes. Using Eq. (1) for the cut-off frequency of a dielectric-filled waveguide [11],

$$f_{\mathrm{c}} = \frac{c_0}{2a\sqrt{\varepsilon_{\mathrm{r}}}}\,, \tag{1}$$

the chosen waveguide width $a = 3.8\,\mathrm{mm}$ leads to a cut-off frequency of 12.3 GHz for the fundamental mode, which is

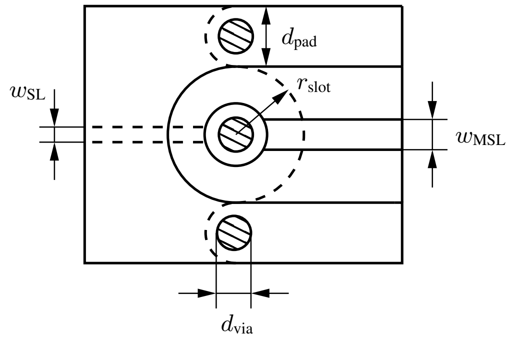

Fig. 4. Top view of the microstrip-to-stripline transition including all design parameters.

TABLE I
FINAL DIMENSIONS OF THE TRANSITION ACCORDING TO FIG. 4.

d_{pad}	d_{via}	h_{sub}	r_{slot}	w_{MSL}	w_{SL}
0.9 mm	0.5 mm	0.635 mm	1.45 mm	0.5 mm	0.2 mm

above the operating frequency of the transition. Additional simulations show that the waveguide mode is attenuated by at least 30 dB within the considered frequency range. The characteristic impedance is almost unaffected by the surrounding ground vias and is 49 Ω according to a separate simulation.

III. Realization and Measurement Results

A. Realization

The proposed transition structure has been fabricated on the dielectric substrate *RT/Duroid 6010* with a permittivity of $\varepsilon_{\mathrm{r}} = 10.2$. The two substrate layers of thickness $h_{\mathrm{sub}} = 0.635\,\mathrm{mm}$ each are joined together using an *RO3001* bonding film.

Fig. 4 illustrates the design parameters of the transition structure introduced in Fig. 1. The top metallization layer consists of a microstrip line of width w_{MSL} and a surrounding ground metallization. Pads with a diameter of d_{pad} are applied to the via holes on every metallization layer. The ground metallization of the microstrip line as well as the stripline of width w_{SL} are situated on the middle layer. The third layer is completely metallized except for a circular clearance of radius r_{slot} around the signal via. The final dimensions used for fabrication are given in Table I.

In order to be able to extract the scattering parameters of a single transition, two back-to-back arrangements of different lengths are manufactured as shown in Fig. 5. Additionally, a single open-ended transition is fabricated to de-embed the transition for circuits based on that transition by applying a TRL calibration technique.

B. Measurement Results

The characteristics of a single microstrip-to-stripline transition are calculated from the measured results for the presented back-to-back arrangements. Using a separate microstrip TRL calibration substrate, the effect of the SMA connector could be compensated. The obtained results are plotted in Fig. 6

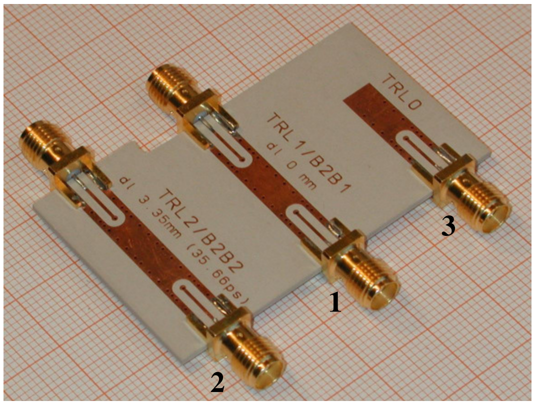

Fig. 5. Photograph of two back-to-back arrangements of the microstrip-to-stripline transition (1+2) and a single open-ended transition (3).

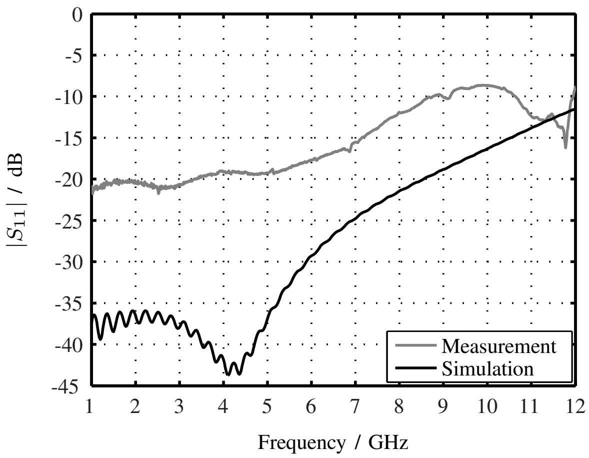

Fig. 6. Simulated and measured return loss of the transition.

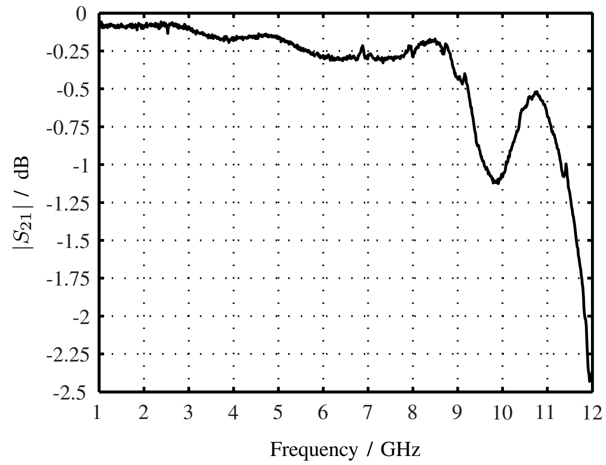

Fig. 7. Measured insertion loss of the transition.

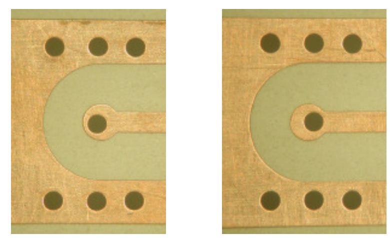

(a) Example 1 (b) Example 2

Fig. 8. Micrographs of the realized transition demonstrating the different via offsets.

and Fig. 7. The reflection coefficient is around -20 dB for frequencies below 5 GHz and increases up to -8.7 dB at 9.8 GHz. The corresponding insertion loss at this frequency is 1.2 dB (see Fig. 7). A comparison to the simulated return loss performance shows a distinct difference between the measured and simulated results. While both curves of $|S_{11}|$ are generally increasing with frequency, the measured return loss is about 10 dB-15 dB higher in the frequency range up to 10 GHz.

The reason for this difference might be found in unavoidable fabrication tolerances, most notably regarding the placement of the via holes. Fig. 8 shows two micrographs of two different fabricated transitions. Different offsets of the signal via can be seen clearly. However, additional simulations have shown that a via offset would only lead to a slight increase of the return loss. Because of the fabrication tolerances, the four transitions of the two back-to-back arrangements are not identical, which leads to an inaccuracy of the de-embedding of a single transition. Besides the effects of other fabrication tolerances like a slight misalignment of the two substrate layers, the influence of the bonding film is probably a main reason for the observed difference between simulated and measured values. The bonding film was neglected in the simulations, which is critical due to its significantly lower permittivity of $\varepsilon_r = 2.28$ in contrast to the permittivity of the surrounding substrate of 10.2.

IV. Application of the Transition

Apart from antenna feeding, one application of the proposed transition is a delay line in stripline technique. Here, the microstrip-to-stripline transition is needed in order to connect the delay line to an SMA connector or the output of a monolithic integrated circuit. In Fig. 10 a photograph of a meander-shaped delay line with a length of 470 mm implemented on a 42 mm $\times$ 42 mm substrate is presented. The line length corresponds to a delay of ca. 5 ns. In this design, via holes are placed also around the stripline in order to prevent the propagation of parallel-plate modes.

The measured scattering parameters of this delay line are plotted in Fig. 10. Here, the transition from coaxial line to microstrip line has been compensated by a TRL calibration. It can be seen that the return loss of the overall structure is predominantly determined by the microstrip-to-stripline transition, especially for high frequencies. The insertion loss of the delay line is increasing with frequency due to dielectric losses of the substrate. The slight drops about every 2 GHz along the course of the transmission coefficient are caused by resonances occurring between the bends of the meander-shaped transmission line.

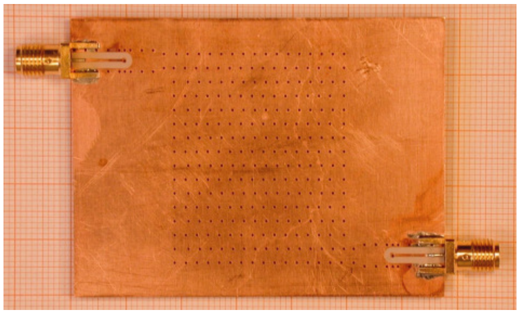

Fig. 9. Photograph of a meander-shaped delay line in stripline technique with the applied microstrip-to-stripline transition.

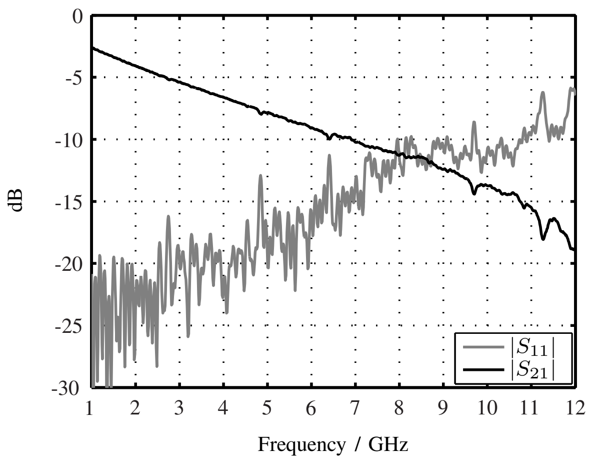

Fig. 10. Scattering parameters of the delay line in stripline technique including the transition to microstrip line.

As mentioned before, the advantage of a stripline design is its frequency-independent group delay as a result of the propagating TEM mode. A transmission line with a constant group delay in a wide frequency range leads to a low dispersion and is therefore suited for the transmission of UWB impulses. Fig. 11 shows the measured group delay over frequency of the meander-shaped delay line. A low group delay variation of ± 28 ps in the FCC frequency range qualifies the transmission line for the application in UWB radar systems.

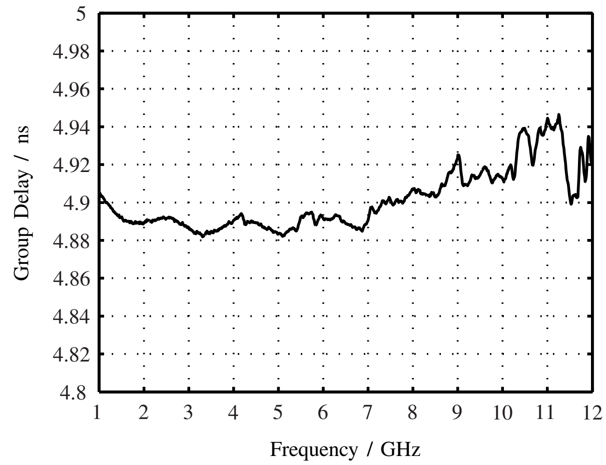

Fig. 11. Group delay of the delay line including transition to microstrip line.

With a meander-shaped delay line in stripline technique, an application of the transition has been presented. The group delay of this transmission line is about 5 ns with a variation of only ± 28 ps.

V. Conclusion

An easy-to-fabricate vertical transition from microstrip to stripline in PCB technology has been presented. Measurements of a manufactured prototype have shown a return loss better than 8.7 dB and an insertion loss better than 1.2 dB throughout the FCC UWB frequency range. The influence of the via pads on the structure's return loss has been examined and simulations have shown that a performance enhancement would be achievable if smaller pads around the via holes would be applied.

Acknowledgment

This work has been funded by the German Research Foundation (DFG) under the program UKoLoS.

References

[1] T. Thiasiriphet, M. Leib, D. Lin, B. Schleicher, J. Lindner, W. Menzel, and H. Schumacher, "Investigations on a comb filter approach for IR-UWB systems," *Frequenz*, vol. 63, no. 9–10, pp. 179–182, Oct. 2009.

[2] G. L. R. C. Marchais and A. Sharaiha, "Stripline slot antenna for UWB communications," *IEEE Antennas and Wireless Propagation Letters*, vol. 5, no. 1, pp. 319–322, Dec. 2006.

[3] M. Leib, M. Frei, D. Sailer, and W. Menzel, "Design and characterization of a UWB slot antenna optimized for radiation in human tissue," in *IEEE International Conference on Ultra-Wideband*, Sep. 2009, pp. 159–163.

[4] H.-H. Jhuang and T.-W. Huang, "Design for electrical performance of wideband multilayer LTCC microstrip-to-stripline transition," in *Electronics Packaging Technology Conference (EPTC)*, Dec. 2004, pp. 506–509.

[5] R. Valois, D. Baillargeat, S. Verdeyme, M. Lahti, and T. Jaakola, "High performances of shielded LTCC vertical transitions from DC up to 50 GHz," *IEEE Transactions on Microwave Theory and Techniques*, vol. 53, no. 6, pp. 2026–2032, Jun. 2005.

[6] Y. C. Lee and C. S. Park, "A novel cpw-to-stripline vertical via transition using a stagger via structure and embedded air cavities for V-band LTCC SiP applications," in *Asia Pacific Microwave Conference (APMC)*, vol. 2, Dec. 2005.

[7] J. Kim, H.-Y. Lee, and T. Itoh, "Novel microstrip-to-stripline transitions for leakage suppression in multilayer microwave circuits," in *IEEE Topical Meeting on Electrical Performance of Electronic Packaging*, Oct. 1998, pp. 252–255.

[8] T. Kushta, K. Narita, T. Kaneko, T. Saeki, and H. Tohya, "Resonance stub effect in a transition from a through via hole to a stripline in multilayer PCBs," vol. 13, no. 5, pp. 169–171, May 2003.

[9] A. Stark and A. F. Jacob, "A broadband vertical transition for millimeter-wave applications," in *European Microwave Conference (EuMC)*, Oct. 2008, pp. 476–479.

[10] *Microwave Studio*, CST - Computer Simulation Technology, 2009.

[11] N. Marcuvitz, *Waveguide Handbook*, ser. 21, IEE Electromagnetic Waves Series. Stevenage: Peter Peregrinus Ltd., 1986.